Colloidal Suspensions of Functionalized Mesoporous Silica Nanoparticles

Johannes Kobler,[†] Karin Möller,[‡] and Thomas Bein[†,*]

[†]Department of Chemistry and Biochemistry and Center for NanoScience (CeNS), University of Munich, Butenandtstrasse 5-13 (E), D-81377 Munich, Germany, and [‡]NanoScape AG, Munich, Germany

ABSTRACT The synthesis and characterization of colloidal mesoporous silica (CMS) functionalized with vinyl-, benzyl-, phenyl-, cyano-, mercapto-, aminopropyl- or dihydroimidazole moieties is reported. Uniform mesoporous particles ranging in size from 40 to 150 nm are generated in a co-condensation process of tetraethylorthosilicate (TEOS) and organotriethoxysilanes (RTES) in alkaline aqueous media containing triethanolamine (TEA) in combination with cetyltrimethylammonium chloride (CTACl) serving as a structure-directing agent. The materials are obtained as colloidal suspensions featuring long-term stability after template removal by ion exchange with an ethanolic solution of ammonium nitrate or HCl. The spherical particles exhibit a wormlike pore system with defined pore sizes and high surface areas. Samples are analyzed by a number of techniques including TEM, SEM, DLS, TGA, Raman, and cross-polarized ^{29}Si-MAS NMR spectroscopy, as well as nitrogen sorption measurements. We demonstrate that co-condensation and grafting methods result in similar changes in the nitrogen adsorption behavior, indicating a successful internal lining of the pores with functional groups through both procedures.

KEYWORDS: colloidal suspension · mesoporous silica · functionalization · co-condensation · nanosized

Various synthetic methods have been developed for the preparation of periodic mesoporous materials,[1] leading to different types of morphologies such as spheres,[2] fibers[3] or vesicles.[4] The large internal surface of these materials can be modified following two main strategies, that is, postsynthesis functionalization (grafting)[5,6] or *in situ* functionalization (co-condensation),[7–9] thus extending the use of mesoporous materials to a wide range of applications.[10] Compared to the modification by grafting, the co-condensation reaction can be expected to improve the degree of bonding between the organic groups and the pore walls and to result in a more homogeneous distribution of the organic groups throughout the pore structure.[11]

Common synthesis routes for mesoporous silica materials lead to particles with typical diameters of 500 nm to several micrometers. The synthesis of nanosized mesoporous materials has only recently received attention. Such mesoporous nanoparticles offer interesting features that are useful in a number of applications such as chemical sensors,[12] chromatography,[13] catalysis,[14] drug delivery,[15] or polymer fillers.[16] If the particles are homogeneously dispersed in a solvent, these colloidal suspensions exhibit unique properties such as optical transparency. Furthermore, the utilization of very small particles improves the mass transfer of molecules into or out of the pore system. The molecular functionalization of the large internal surface of these materials can extend the range of possible applications, for example, toward selective (ad)sorption or specific catalytic activity.

The preparation of nanosized particles can be realized through various methods. Brinker *et al.* described an aerosol-based process resulting in a solid dry product.[17] Another strategy utilizes the addition of a nonionic surfactant as a suppressant of particle growth through encapsulation, leading to a gel of agglomerated small particles.[18] Amoros *et al.*[19] presented a facile method leading to nanosized mesoporous silica using water, tetraethylorthosilicate (TEOS), and cetyltrimethylammonium cations in combination with triethanolamine (TEA) which is supposed to act as a hydrolysis-retarding agent. However, the final product of this procedure is a gel of fused particles which cannot be redispersed.

There are only few publications describing synthesis methods that lead to colloidal suspensions of periodic mesoporous materials.[20–24] Their synthesis typically relies on procedures applying high dilutions; this can result in time-consuming subsequent processing steps. For instance, truly colloidal suspensions of well-defined mesoporous particles were obtained by Mann *et al.*[25,26] by diluting and quenching the

*Address correspondence to bein@lmu.de.

Received for review April 14, 2007 and accepted February 01, 2008.

Published online March 22, 2008.
10.1021/nn700008s CCC: $40.75

TABLE 1. Type and Amount of Functionalized Organotriethoxysilane Used in the Co-condensation

sample	RTES	M (g mol^{-1})	n (mmol)	m (g)
CMS-VI	vinyltriethoxysilane	190.3	2	0.381
CMS-PH	phenyltriethoxysilane	240.4	2	0.481
CMS-BZ	benzyltriethoxysilane	254.4	2	0.509
CMS-CP	3-cyanopropyltriethoxysilane	231.4	2	0.463
CMS-MP	3-mercaptopropyltriethoxysilane	238.4	2	0.477
CMS-AP-c[a]	3-aminopropyltriethoxysilane	221.4	0.65	0.144
CMS-IM[a]	4,5-dihydroimidazolepropyltriethoxysilane	274.4	0.65	0.178

[a]Synthesized following procedure b.

condensation reaction of TEOS in aqueous alkaline solution with a large excess of water. They could manipulate the particle size by varying the time interval for quenching. In a recent publication, Rathousky *et al.*[21] also describe a method for the preparation of colloidal MCM-41, working with even higher dilutions. We have recently presented a method utilizing the polyalcohol triethanolamine that results in nonaggregated, colloidal suspensions of mesoporous silicas (CMS) from concentrated solutions.[23] Round particles with wormhole structures and diameters of about 100 nm with very narrow particle size distributions were obtained in the form of stable suspensions. Tuning the reaction conditions allowed us to control particle size down to 50 nm. Colloidal stability was even sustained after template extraction, which resulted in surface areas of about 1000 $m^2\ g^{-1}$. Extraction of the template, in contrast to calcination, is the method of choice when organic moieties are introduced in the wall structure by a co-condensation procedure. Our previous work thus provides a general basis for studying surface modifications in nanosized, colloidal mesoporous particles. We have further demonstrated that this approach can be applied for the functionalization of CMS particles by inclusion of mercapto-residues into the pore walls.[24]

Here we extend the above synthesis methods toward the generation of functionalized, hydrophilic as well as hydrophobic colloidal mesoporous silica with high yields. As described in the following, various alkoxysilanes bearing organic moieties can be incorporated into the pores of the colloidal nanoparticles using this general method.

RESULTS AND DISCUSSION

Colloidal mesoporous silica was prepared in the form of nonfunctionalized pure-silica MCM-like material (CMS) and as functionalized mesoporous materials carrying seven different organic groups (R) in the pore walls (CMS-R; see Table 1). The materials were obtained as colloidal suspensions with relatively uniform particle sizes between 40 and 150 nm. Tetraethylorthosilicate (TEOS) and organotriethoxysilanes (RTES) form the MCM-like material in combination with cetyltrimethylammonium cations ($CTMA^+$) as structure directing agent in a co-condensation process (Figure 1).

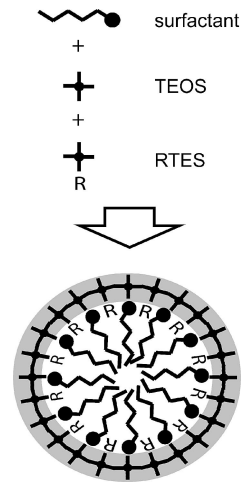

Figure 1. Scheme of the co-condensation reaction of alkoxysilanes with a micelle-forming surfactant.

This S^+I^- assembly takes place in an alkaline aqueous medium, with triethanolamine (TEA) as basic reactant. TEA can also act as a complexing agent that retards the hydrolysis of the alkoxides.[27–29] We assume that in these reactions the uncomplexed TEOS is hydrolyzed upon contact with water, followed by forming the seeds of the mesostructure. The large excess of TEA probably keeps the seeds separated from each other during the condensation process giving rise finally to a large number of particles with relatively small diameters.

The morphology and particle size of the synthesized materials was analyzed with dynamic light scattering (DLS) and electron microscopy (TEM and SEM). In the TEM micrographs we observe discrete, near-spherical particles with a disordered, wormlike pore arrangement with either synthesis procedure a or b, differing substantially in the amount of TEA added in the synthesis (see Experimental section).[23] The particles show a narrow particle size distribution with a polydispersion index (PDI) of around 0.1. This narrow size distribution is maintained after extraction of the template by an ion-exchange method using an ethanolic solution of ammonium nitrate (Figure 2).

The synthesis procedure developed for pure siliceous nanoparticles was extended toward a simulta-

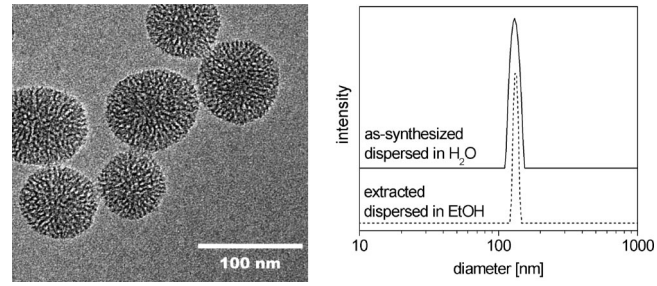

Figure 2. TEM-micrograph and particle size distribution of sample CMS-1 determined by dynamic light scattering.

TABLE 2. Properties of Colloidal Mesoporous Materials As Analyzed with Different Methods[a]

	particle size		TGA data	N_2 sorption data		
sample	diameter DLS (nm)	diameter TEM (nm)	T at DTG_{max} (°C)	surface area ($m^2\ g^{-1}$)	pore volume at $p/p_0 < 0.8$ ($cm^3\ g^{-1}$)	pore diameter[b] (nm)
CMS-1	100	80–120	-	1150	1.0	2.8
CMS-VI	120	50–100	290	1230	0.74	2.0
CMS-CP	130	80–150	350	1200	0.72	2.2
CMS-MP	90	50–70	350	970	0.63	2.3
CMS-PH	80	40–60	610	1040	0.73	1.8
CMS-BZ	110	50–100	470	1120	0.65	1.6
CMS-2	160	80–130	-	930	0.82	2.7
CMS-AP-g	170	80–130	305	780	0.51	2.2
CMS-IM	130	na	340	220	0.17	2.4

[a]Samples are modified via co-condensation with vinyl-(CMS-VI), benzyl-(CMS-BZ), phenyl-(CMS-PH), cyanopropyl-(CMS-CP), mercaptopropyl-(CMS-MP), and aminopropyl-(CMS-AP-c), as well as dihydroimidazolepropyl(CMS-IM) groups. CMS-AP-g: sample CMS-2 grafted with APTES. [b]Pore diameter was determined with the BJH method from the desorption branch.

neous reaction of TEOS and a variety of organotriethoxysilane precursors to obtain functionalized surfaces. Hybrid mesoporous materials incorporating the following organic groups, namely, vinyl-(CMS-VI), benzyl-(CMS-BZ), phenyl-(CMS-PH), cyanopropyl-(CMS-CP), mercaptopropyl-(CMS-MP), and aminopropyl-(CMS-AP), as well as dihydroimidazolepropyl-(CMS-IM) residues were thus synthesized. The different nanoscale mesoporous materials are listed in Table 2. These surface-modified mesoporous organosilicas often show an even narrower size distribution than the pure silica parent materials (Figure 3).

The observed mean particle size obtained from DLS measurements varies in most cases from about 80 to 150 nm, depending on the incorporated functional group and the synthesis method employed. The particle size observed with electron microscopy is often slightly smaller than the hydrodynamic diameter measured by DLS. This observation can be explained with occasional weak aggregation of the particles. The discrepancy is seen clearly in the case of the organically modified materials, especially, if hydrophobic aromatic groups such as phenyl residues are incorporated in the structure (Table 2).

The products with incorporated organic groups, especially CMS-PH or CMS-MP, appear as nearly perfect spheres with diameters of about 50 nm. The narrow particle size distribution of the mesoporous materials can also be confirmed with scanning electron microscopy (Figure 4). Here, a stable colloidal suspension of extracted CMS-BZ was used for spin-coating a gold-sputtered glass plate resulting in a homogeneous coverage of mesoporous particles. The benzyl-modified mesoporous spheres have diameters in the range of 50 to 80 nm.

However, organosilane reagents with basic character strongly influenced the morphology when a co-condensation synthesis was performed. When 3-aminopropyltriethoxysilane (APTES) was added to the reaction mixture at a molar ratio of 10 TEOS: 1 (APTES) following synthesis route b, we observed a large increase in particle size. Particle diameters between 250 to 400 nm were obtained as opposed to only 45–60 nm in a corresponding synthesis without (APTES) present. As seen in Figure 5, near spherical particles with a wormhole pore arrangement similar to the non-functionalized samples are still present. This suspension of larger particles showed a partial sedimentation with time. To avoid this behavior, we used an alternative procedure for sample preparation by grafting the amino groups into the pores of a premade mesoporous silica support using synthesis b (TEOS: TEA = 1:4). Accessibility of the precursor pores was achieved through prior template extraction, which resulted in a surface area of 930 $m^2\ g^{-1}$ (sample CMS-2, see Table 2). Using this approach, the morphology and particle size (TEM: 80–130 nm; DLS: *ca.* 160 nm) of the precursor was now unchanged after functionalization (see Figure 6).

An influence of organic functional surface groups upon the morphology of mesoporous materials was also observed by Huh *et al.*[9] They found a strong in-

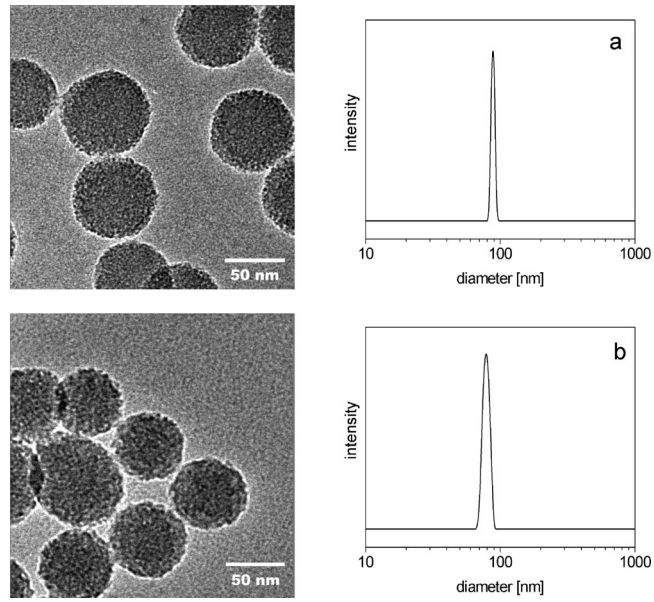

Figure 3. TEM micrographs and particle size distributions calculated from DLS-data of samples CMS-MP (a) and CMS-PH (b).

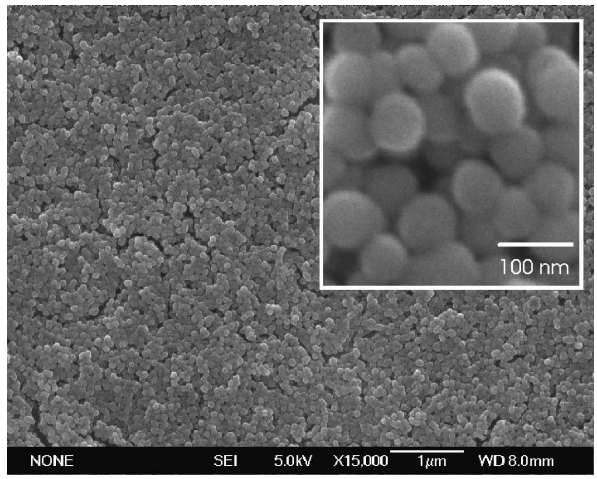

Figure 4. SEM-micrograph of a mesoporous film prepared by spin-coating, using a colloidal suspension of CMS-BZ.

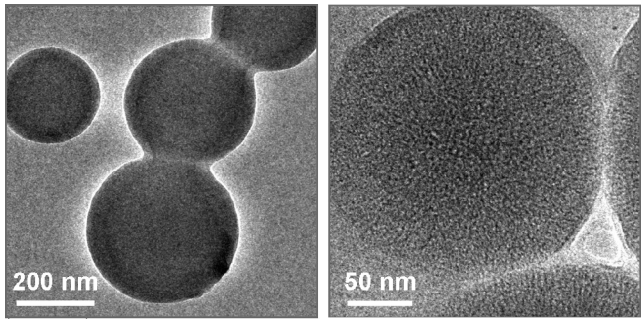

Figure 5. TEM of sample CMS-AP-c (co-condensed).

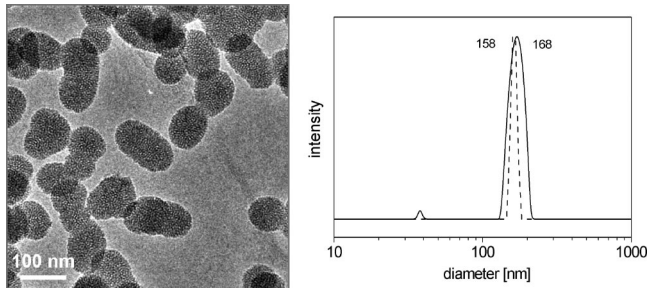

Figure 6. (a) TEM of sample CMS-AP-g (grafted) and (b) DLS in EtOH, before (dotted line) and after (full line) grafting with APTES.

crease of the particle size when using hydrophilic organosilanes, especially with amino-containing residues, while hydrophobic residues stimulated the formation of smaller particles. They concluded that hydrophobic groups are able to align with the organic tails of the template, while hydrophilic residues would disturb the Gouy–Chapman region thus causing a different growth behavior. Our results support their findings for the hydrophobic functional groups. Furthermore, the organosilanes with basic character led to comparable results: we observe an increase in size with the aminopropyl as well as the propyl-4,5-dihydroimidazole group. In contrast, weakly acidic mercapto residues stimulate the formation of even smaller spherical particles compared to the nonfunctionalized parent compound, as long as a synthesis procedure with TEA is applied.[24]

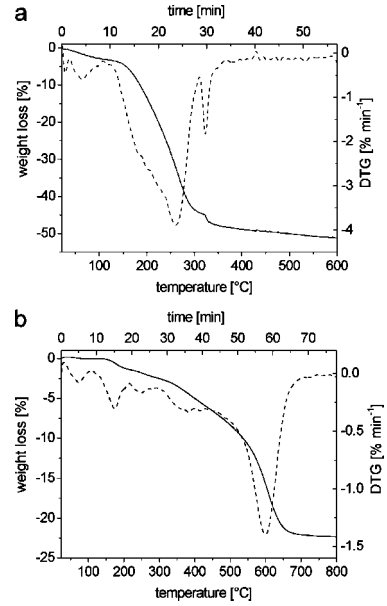

Figure 7. Thermogravimetric analysis (TG-DTG) of washed CMS-1 with template (a), and phenyl modified, extracted mesoporous silica CMS-PH (b).

The presence of the organic functional groups can be verified with several methods. Thermogravimetric analysis (TGA) shows the decomposition behavior during the heating of the samples in air. The decomposition temperature, more precisely the temperature when the first derivative of the weight loss reaches a maximum, varies over a rather wide range for the different functional groups (Figures 7 and 8). Figure 7a shows the weight loss of the washed nonfunctionalized sample

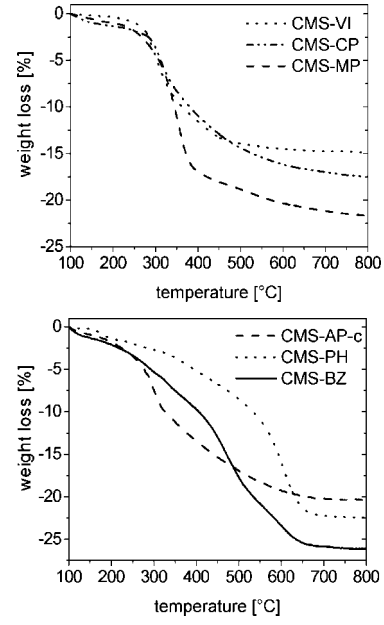

Figure 8. Thermogravimetric analysis of the surface-modified and extracted mesoporous silica materials (starting at 100 °C to compensate for different water losses).

CMS-1, still containing the template inside the pores with a maximum around 250 °C. This decomposition process of the template is completed well before the decomposition of the phenyl-residue in sample CMS-PH starts. Figure 7b shows the decomposition of this group around a temperature of 600 °C in a sample that was previously template-extracted. This extreme stability is not observed for the other functional groups. They start to decompose at a lower temperature, which makes a clear separation from the degradation of the template difficult (Figure 8). However, when nonfunctionalized samples were analyzed with TGA after template extraction we still observed a weight loss of around 4–7 wt % between 100–500 °C. About 3% weight loss can be accounted for by residual template fragments that were detected by elemental analysis of nonfunctionalized samples. Additionally, the dehydroxylation of surface hydroxyl groups should be considered. Usually up to 3 SiOH groups per nm^2 are found in mesoporous materials.[22,30] With surface areas of about 1000 m^2 g^{-1} one can estimate a maximum 5 wt% loss due to water release from these samples by dehydroxylation.

This loss must be taken into account when the amount of organic residue is determined from TGA measurements. Usually we find a TGA-weight loss between 15–25 wt % in template-extracted functionalized samples (above 100 °C). For example, elemental analysis of grafted CMS-AP-g gave a content (by weight) of 2.85% for nitrogen in these samples, which would correspond to 12 wt % propylamine residue in the sample. In comparison, the loss observed in the TGA for CMS-AP-g was 15%. The small difference may be due to dehydroxylation and residual template.

The connectivity of the functional organic groups to the silica framework is best demonstrated by cross-polarized ^{29}Si-MAS NMR spectroscopy (Figure 9). The spectra show peaks at –110 ppm (Q^4) and –102 ppm (Q^3) [Q^n = $Si(OSi)_n(OH)_{4-n}$], n = 2–4, representing the fully condensed silica and silica with one terminal hydroxyl group. Geminal hydroxyls are barely present in these samples (resonance at –92 ppm; Q^2). One or two additional peaks are observed owing to the T^2 and T^3 resonances of the incorporated organosiloxanes [T^m = $RSi(OSi)_m(OH)_{3-m}$], m = 2–3, at values commonly observed in functionalized mesoporous materials. Propyl-bridged functional groups display shifts around −67 and −60 ppm, while directly bound residues with C═C bonds show resonances at more negative values (Table 3).[9] The prevalence of the T^3 peak, that is, the 3-fold coordination of the siloxane indicates (near) complete condensation of the functional groups into the wall structure of the nanoparticles. It is interesting to note that only in the grafted amino-functionalized sample CMS-AP-g do we see a strong reduction of the relative intensity of the Q^3 signal. This points to the difference in synthesis procedure, which exploits the terminal hydroxyls for anchoring in the case of grafting. Covalent bonding is still achieved by this method to a great extent by 3-fold coordination to the silica wall or within the newly grafted silica-containing monolayer.

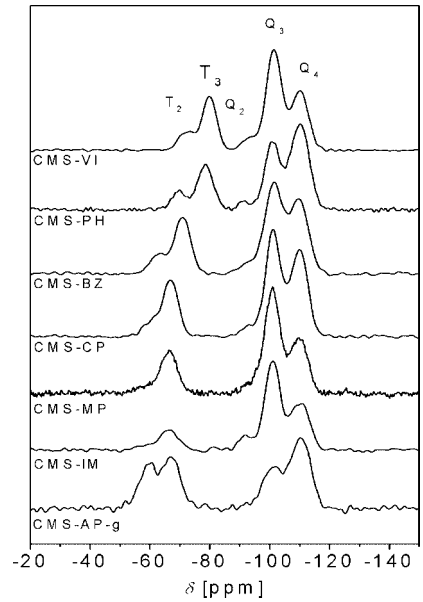

Figure 9. Cross-polarized ^{29}Si-MAS NMR spectra of the functionalized mesoporous materials.

The characteristic vibrational modes of the incorporated functional groups are clearly displayed in their Raman spectra, which are not obscured by hydroxyl vibrations of the host as in IR spectroscopy (Figure 10). Intensive peaks of the phenyl- and benzyl-substituted samples CMS-PH and CMS-BZ, originating from the in-plane C−H deformation vibrations of the aromatic ring, are seen at about 1000 cm^{-1}. Additionally, these samples show the typical peaks for aromatic C−H and ring C═C stretching vibrations at 3060 and 1590 cm^{-1}, respectively.[31] Similar Raman bands are observed for the propylene-bridged imidazole CMS-IM sample. The signal for the C═N ring vibration of this sample is shifted from 1610 cm^{-1} in the liquid precursor to 1660 cm^{-1} and substantially broadened. Both features might point to the spatial confinement of this voluminous group. This ring vibration is also clearly observed at 1650 cm^{-1} in the IR spectrum (not shown). A similar frequency was observed in imidazole-functionalized SBA mesoporous materials.[32] In the vinyl-modified sample

TABLE 3. Cross-Polarized ^{29}Si-MAS NMR Spectroscopy Data of Functionalized Mesoporous Materials

sample	chemical shift			
	Q^4	Q^3	T^3	T^2
CMS-VI	−110	−101	−80	−73
CMS-PH	−110	−101	−79	−70
CMS-BZ	−110	−101	−71	−63
CMS-CP	−110	−101	−67	−58
CMS-MP	−110	−101	−67	
CMS-IM	−110	−101	−67	
CMS-AP-g	−110	−101	−67	−60

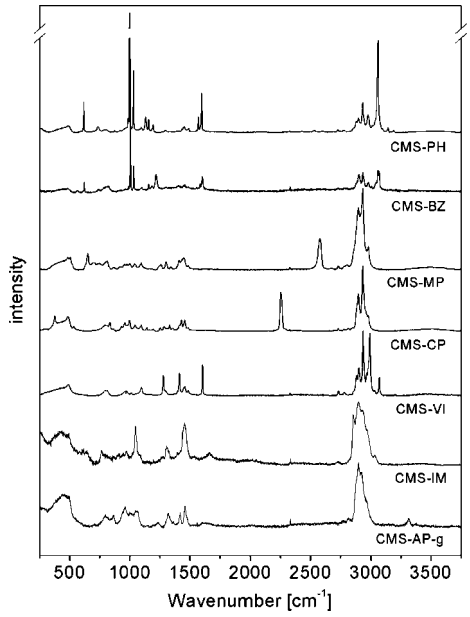

Figure 10. Raman spectra of template-extracted functionalized mesoporous materials.

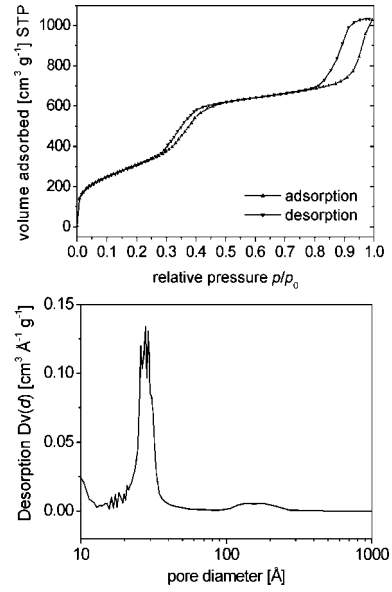

Figure 11. Nitrogen sorption isotherm (top) and pore size distribution (bottom) according to the BJH theory of mesoporous silica CMS-1.

(CMS-VI) we find the alkene C−H vibrations and the C═C stretching vibrations at 3070 and 1605 cm^{-1}, respectively. The nitrile group of CMS-CP causes a characteristic narrow band at 2250 cm^{-1}. The typical peak for the S−H group in the mercaptopropyl-containing CMS-MP occurs at 2580 cm^{-1}, and additionally we find a band at 657 cm^{-1} due to the C−S vibration. Both Raman bands indicate that the mercapto groups are intact and that no disulfide bridges have formed.[33] Direct spectroscopic evidence for the amino group in the sample CMS-AP-g is difficult to obtain. We can identify a broad band between 1600 and 1680 cm^{-1}, which is not present in the template-extracted, nonfunctionalized sample. Additionally, we can identify the aminopropyl-group through several bands that are neither present in template-containing nor template-extracted nonfunctionalized samples: the NH_2 wagging band at 864 cm^{-1}, the NH_2 twisting at 1233 cm^{-1}, and the NH_2 stretch vibrations at 3315 and 3377 cm^{-1}.

After extraction of the surfactant, most of the functionalized porous materials show high surface areas and pore volumes. The sorption properties were determined using nitrogen adsorption–desorption at 77 K. In case of the unmodified materials CMS-1 or -2, a typical type IV isotherm with a clear hysteresis from filling of the cylindrical pores is observed. Textural pores of ~20 nm, originating from the closely packed nanospheres in the powders are visible above a relative pressure of 0.8 p/p_0. The entire surface area calculated according to the BET-theory is 1150 $m^2\ g^{-1}$ for CMS-1. The product exhibits a high pore volume of 1 $cm^3\ g^{-1}$ and a narrow pore size distribution with an average diameter of 2.8 nm as determined with the BJH method (this method is believed to underestimate the pore size by about 1 nm) (Figure 11).[34] Calcined CMS-1 shows an even higher surface area of 1400 $m^2\ g^{-1}$ with pore volumes of 1.1 $cm^3\ g^{-1}$.

The type of adsorption isotherm is unchanged in the functionalized nanosized materials, and the inclusion of the functional groups does not significantly affect the overall surface area of the materials, provided co-condensation is performed following synthesis procedure a (Table 2). However, a significant reduction of the pore volume and particularly the pore size give a strong indication for a successful lining of the pores with the organic residues (Figure 12).

To some extent the size of the functional groups influences the shrinkage of the pore diameter (all diameters according to BJH theory). While the unmodified

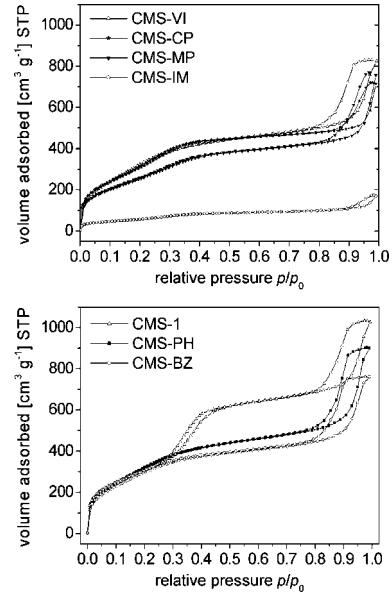

Figure 12. Nitrogen sorption isotherms of reference and co-condensed materials, respectively.

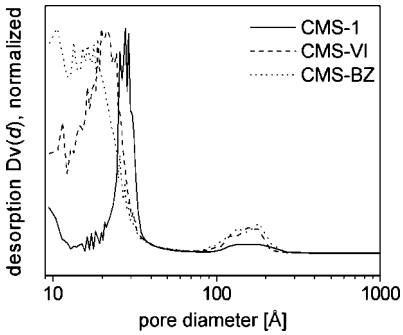

Figure 13. Changes in the pore size distribution with increasing size of the incorporated organic moieties in mesoporous silica.

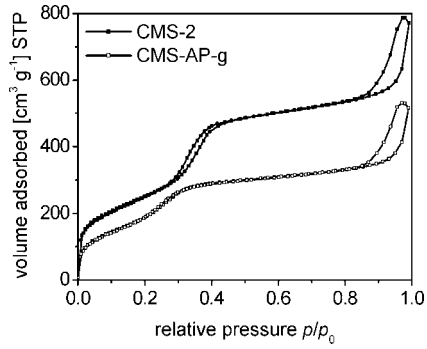

Figure 14. Nitrogen sorption before (CMS-2) and after grafting with aminopropyltriethoxysilane (CMS-AP-g)

mesoporous silica has an average pore diameter of 2.8 nm, in vinyl-functionalized materials (CMS-VI) we find pores with a mean diameter of 2.0 nm, and the bulky nature of the benzyl group in CMS-BZ causes a reduction to 1.6 nm (Figure 13). Unusually large reductions in pore volume and surface area are observed in sample CMS-IM; this could be related to some pore clogging by residual template. A similar reduction in porosity was also observed upon co-condensation of dihydroimidazole-propyltriethoxysilane in the synthesis of SBA-15.[32]

The changes in adsorption behavior due to the lining of the pores with functional groups can be directly observed when grafting to the preformed pore system is applied instead of a co-condensation synthesis. A nitrogen sorption isotherm comparable to the one of co-condensed samples carrying other functional groups is obtained for the aminopropyl-grafted sample CMS-AP-g (see Figure 14). The shift of the condensation step and the reduction in N_2 uptake indicates the location of the aminopropyl groups inside the pores.

The surface coverage of functional groups in the nanoscale mesoporous samples can be estimated from thermogravimetric measurements in conjunction with the surface area presuming that all organic groups are located on the surface. For example, the weight-loss of CMS-PH due to the decomposition of the organic group is about 20%. The calculated surface area according to BET-theory is 1040 $m^2\ g^{-1}$. From these data, a surface coverage of 2.6 mmol g^{-1} or 1.5 phenyl groups per nm^2 can be calculated. Similarly, a value of 1.6 aminopropyl groups per nm^2 was calculated for the grafted sample CMS-AP-g.

CONCLUSIONS

The synthetic approach presented here can serve as a general method for the preparation of both colloidal mesoporous silica spheres (CMS) and functionalized colloidal suspensions of nanoscale mesoporous materials with high yields from concentrated solutions. Narrow particle size distributions in the range of about 40 to 150 nm were established with dynamic light scattering (DLS) measurements and electron microscopy before and after template extraction. Discrete nanoscale mesoporous particles with functionalized pore surfaces result when adding functional organoalkoxysilanes directly to the initial silica precursor solutions, or alternatively, when organoalkoxysilanes are grafted to the pore surfaces in a second step. The comparison of both methods with nitrogen sorption analysis and spectroscopic data demonstrates that the functional groups are located at the inner surfaces of the mesoporous channel systems, while the latter retain large surface areas and significant pore volumes.

EXPERIMENTAL SECTION

Synthesis. Two slightly different synthesis methods were used, as already described in our recent publication about the synthesis of nanosized pure mesoporous silicates[23] and adapted for functionalization with organic moieties. All chemicals were reagent grade (98% or higher) purchased from Sigma-Aldrich and used without further purification. The water was deionized.

(a) Pure Siliceous CMS-1. 14.3 g (96 mmol) of TEA and 2 mL (9 mmol) of TEOS were combined in a 125 mL polypropylene bottle with a lid. The two-phase mixture was heated in an oil bath at 90 °C for 20 min without stirring. Immediately after the mixture was taken out of the oil bath, 26.7 g of an aqueous solution (2.5% wt) of CTACl which had been heated to 60 °C was added, and the final mixture was stirred (600 rpm) for at least 3 h at 23 °C. The molar composition of CMS-1 is: 0.75 Si/8 TEA/0.17 CTACl/120 H_2O.

Functionalized mesoporous silica CMS-R: 14.3 g (96 mmol) of TEA and a mixture of 2.23 mL (10 mmol) of TEOS plus the corresponding quantity of 2 mmol (Table 1) of organotriethoxysilane (RTES) were combined in a 125 mL polypropylene bottle with lid. The two-phase mixture was heated in an oil bath at 90 °C for 20 min without stirring. Immediately after the mixture was taken out of the oil bath, 26.7 g of an aqueous solution (2.5% wt) of CTACl which had been heated to 60 °C was added and the final mixture was stirred (600 rpm) for at least 3 h at 23 °C. The molar composition of these functionalized materials is 1 Si/8 TEA/0.17 CTACl/120 H2O.

(b) Pure siliceous CMS-2. A stock solution was prepared as follows: 64 mL of water (3.55 mol), 10.5 mL of ethanol (0.179 mol), and 10.4 mL of a 25 wt % CTACl solution (7.86 mmol) were mixed and stirred for 10 min. To the above solution, 16.5 mL (0.124 mol) of TEA was subsequently added, and the mixture was further stirred until all TEA was dissolved, resulting in a pH value of 11.3. Typi-

cally, 20 mL of this stock solution was heated in an oil bath to 60 °C, to which 1.454 mL of TEOS was added dropwise (within 2–3 min) under stirring. A white suspension developed after ten minutes. The suspension was cooled to room temperature after 2 h, at which time the pH had decreased to 9.3. Molar ratios for this route are 1 TEOS/0.27 CTACl/4 TEA/137 H_2O/6.2 EtOH.

Co-condensation (sample CMS-AP-c) with 3-aminopropyl- (APTES) or 4,5-dihydroimidazolepropyltriethoxysilane was achieved by the simultaneous addition of TEOS and the silane in a molar ratio of 10:1 or 1.454 mL of TEOS (6.5 mmol) + 0.152 mL (0.65 mmol) of APTES (or the corresponding amount of dihydroimidazole). A molar ratio of TEOS/TEA of 1:1 was applied here to minimize the particle size (see our former work),[23] resulting in a final molar composition of 1 TEOS/0.1 APTES/0.27 CTACl/1 TEA/137 H_2O/6.2 EtOH.

Grafting (CMS-AP-g): a sample of pure mesoporous silica CMS-2 was taken up into absolute ethanol (<0.02% water) after centrifugation following template extraction. An ethanolic solution of APTES was added to this sample in a molar ratio of 5 Si/1 APTES, and the mixture was stirred at room temperature for 20 h. The sample was finally centrifuged and washed two times in ethanol.

Extraction of template from the mesoporous silica: 50 mL of ethanol were added to the translucent, colloidal aqueous suspension of the mesoporous material. The resulting precipitate was centrifuged for 20 min at 40.000 RCF (g). After decantation, the sediment was redispersed through vigorous stirring in 50 mL of an ethanolic solution of ammonium nitrate (20 g L^{-1}) and then treated for 20 min in an ultrasonic bath (35 kHz). Alternatively the mixture can be refluxed for 1 h. This procedure was repeated until the sediment after centrifugation was completely transparent, normally one or two times. To replace the ammonium ions in the structure, this operation was repeated with a solution of concentrated hydrochloric acid in ethanol (5 g L^{-1}). After it is washed with pure ethanol, the transparent gelatinous cake obtained after centrifugation could be redispersed in ethanol, leading to a colloidal suspension of the extracted product in ethanol.

Methods. Dynamic light scattering (DLS) data were collected with an ALV-NIBS/HPPS high performance particle sizer in PMMA cuvettes at 25 °C. Raman spectroscopy was performed with a He−Ne laser (633 nm) on a LabRAM HR UV–vis (HORIBA Jobin Yvon) Raman microscope (Olympus BX41) equipped with a Symphony CCD detection system. The spectra were baseline-corrected. For thermogravimetric analysis (TGA) 10 mg of dry powder were heated in corundum crucibles from 30 to 800 °C (10 °C min^{-1}) in a flow of synthetic air (25 mL min^{-1}) using a Netzsch STA 449 C Jupiter thermobalance. For the SEM analysis, films were prepared on a gold-covered glass slide by spin-coating, using ethanolic suspensions of the extracted material. Shape and dimensions of the particles were determined with a JEOL JSM-6500F scanning electron microscope (SEM) equipped with an Oxford EDX analysis system. Transmission electron microscopy (TEM) was carried out on a JEOL JEM 2011 instrument with LaB_6 cathode at 200 kV. Samples were prepared on a Plano holey carbon-coated copper grid by evaporating one droplet of diluted ethanolic suspension of the extracted material. Cross-polarized ^{29}Si-MAS NMR measurements were performed on a Bruker DSX Avance500 FT spectrometer in a 4 mm ZrO_2 rotor. The spinning rate was 6 kHz and a total number of 256 scans were recorded. The nitrogen sorption isotherms (77 K) were obtained using a Quantachrome NOVA 4000e Surface Area & Pore Size analyzer. Surface area calculations were made using the Brunauer–Emmett–Teller (BET) equation in the range of $p/p_0 <$ 0.3. Pore-size distributions and pore-volumes were determined using the BJH-method in the range of $p/p_0 <$ 0.8.

Acknowledgment. The authors acknowledge funding from the Bavarian Research Foundation for this project as part of the network FORNANO. We thank Dr. Nikolay Petkov for acquiring the electron micrographs.

REFERENCES AND NOTES

1. Kresge, C. T.; Leonowicz, M. E.; Roth, W. J.; Vartuli, J. C.; Beck, J. S. Ordered Mesoporous Molecular-Sieves Synthesized by a Liquid-Crystal Template Mechanism. *Nature* **1992**, *359*, 710–712.
2. Qi, L. M.; Ma, J. M.; Cheng, H. M.; Zhao, Z. G. Micrometer-Sized Mesoporous Silica Spheres Grown Under Static Conditions. *Chem. Mater.* **1998**, *10*, 1623–1626.
3. Huo, Q. S.; Zhao, D. Y.; Feng, J. L.; Weston, K.; Buratto, S. K.; Stucky, G. D.; Schacht, S.; Schuth, F. Room Temperature Growth of Mesoporous Silica Fibers: A New High-Surface-Area Optical Waveguide. *Adv. Mater. (Weinheim, Ger.)* **1997**, *9*, 974–978.
4. Li, Y. S.; Shi, J. L.; Hua, Z. L.; Chen, H. R.; Ruan, M. L.; Yan, D. S. Hollow Spheres of Mesoporous Aluminosilicate with a Three-Dimensional Pore Network and Extraordinarily High Hydrothermal Stability. *Nano Lett.* **2003**, *3*, 609–612.
5. Cauvel, A.; Renard, G.; Brunel, D. Monoglyceride Synthesis by Heterogeneous Catalysis Using MCM-41 Type Silicas Functionalized with Amino Groups. *J. Org. Chem.* **1997**, *62*, 749–751.
6. Zhao, X. S.; Lu, G. Q. Modification of MCM-41 by Surface Silylation with Trimethylchlorosilane and Adsorption Study. *J. Phys. Chem. B* **1998**, *102*, 1556–1561.
7. Burkett, S. L.; Sims, S. D.; Mann, S. Synthesis of Hybrid Inorganic−Organic Mesoporous Silica by Co-condensation of Siloxane and Organosiloxane Precursors. *Chem. Commun. (Cambridge, U.K.)* **1996**, 1367–1368.
8. Burleigh, M. C.; Markowitz, M. A.; Spector, M. S.; Gaber, B. P. Direct Synthesis of Periodic Mesoporous Organosilicas: Functional Incorporation by Co-condensation with Organosilanes. *J. Phys. Chem. B* **2001**, *105*, 9935–9942.
9. Huh, S.; Wiench, J. W.; Yoo, J.-C.; Pruski, M.; Lin, V. S.-Y. Organic Functionalization and Morphology Control of Mesoporous Silicas via a Co-condensation Synthesis Method. *Chem. Mater.* **2003**, *15*, 4247–4256.
10. Anwander, R. SOMC@PMS. Surface Organometallic Chemistry at Periodic Mesoporous Silica. *Chem. Mater.* **2001**, *13*, 4419–4438.
11. Diaz, I.; Mohino, F.; Perez-Pariente, J.; Sastre, E. Study by TG-MS of the Oxidation of SH-MCM-41 to SO_3H-MCM-41. *Thermochim. Acta* **2004**, *413*, 201–207.
12. Qi, Z.-M.; Honma, I.; Zhou, H. Ordered-Mesoporous-Silica-Thin-Film-Based Chemical Gas Sensors with Integrated Optical Polarimetric Interferometry. *Appl. Phys. Lett.* **2006**, *88*, 053503/1–053503/3.
13. Boissiere, C.; Kummel, M.; Persin, M.; Larbot, A.; Prouzet, E. Spherical MSU-1 Mesoporous Silica Particles Tuned for HPLC. *Adv. Funct. Mater.* **2001**, *11*, 129–135.
14. Ren, J.; Ding, J.; Chan, K.-Y.; Wang, H. Dual-Porosity Carbon Templated from Monosize Mesoporous Silica Nanoparticles. *Chem. Mater.* **2007**, *19*, 2786–2795.
15. Lu, J.; Liong, M.; Zink, J. I.; Tammanoi, F. Mesoporous Silica Nanoparticles as a Delivery System for Hydrophobic Anticancer Drugs. *Small* **2007**, *3*, 1341–1346.
16. Asai, S.; Tominaga, Y.; Sumita, M. Mesoporous Silica as Inorganic Filler in Polymer Composites. *Zeoraito* **2006**, *23*, 117–124.
17. Lu, Y. F.; Fan, H. Y.; Stump, A.; Ward, T. L.; Rieker, T.; Brinker, C. J. Aerosol-Assisted Self-Assembly of Mesostructured Spherical Nanoparticles. *Nature* **1999**, *398*, 223–226.
18. Suzuki, K.; Ikari, K.; Imai, H. Synthesis of Silica Nanoparticles Having a Well-Ordered Mesostructure Using a Double Surfactant System. *J. Am. Chem. Soc.* **2004**, *126*, 462–463.
19. El Haskouri, J.; Ortiz de Zarate, D.; Guillem, C.; Beltran-Porter, A.; Caldes, M.; Marcos, M. D.; Beltran-Porter, D.; Latorre, J.; Amoros, P. Hierarchical Porous Nanosized Organosilicas. *Chem. Mater.* **2002**, *14*, 4502–4504.
20. Nooney, R. I.; Thirunavukkarasu, D.; Chen, Y.; Josephs, R.; Ostafin, A. E. Synthesis of Nanoscale Mesoporous Silica Spheres with Controlled Particle Size. *Chem. Mater.* **2002**, *14*, 4721–4728.
21. Rathousky, J.; Zukalova, M.; Kooyman, P. J.; Zukal, A. Synthesis and Characterization of Colloidal MCM-41. *Colloids Surf., A* **2004**, *241*, 81–86.
22. Cai, Q.; Luo, Z. S.; Pang, W. Q.; Fan, Y. W.; Chen, X. H.; Cui, F. Z. Dilute Solution Routes to Various Controllable Morphologies of MCM-41 Silica with a Basic Medium. *Chem. Mater.* **2001**, *13*, 258–263.

23. Moeller, K.; Kobler, J.; Bein, T. Colloidal Suspensions of Nanometer-Sized Mesoporous Silica. *Adv. Funct. Mater.* **2007**, *17*, 605–612.
24. Moeller, K.; Kobler, J.; Bein, T. Colloidal Suspensions of Mercapto-Functionalized Nanosized Mesoporous Silica. *J. Mater. Chem.* **2007**, *17*, 624–631.
25. Fowler, C. E.; Khushalani, D.; Lebeau, B.; Mann, S. Nanoscale Materials with Mesostructured Interiors. *Adv. Mater. (Weinheim, Ger.)* **2001**, *13*, 649–652.
26. Sadasivan, S.; Khushalani, D.; Mann, S. Synthesis and Shape Modification of Organo-Functionalized Silica Nanoparticles with Ordered Mesostructured Interiors. *J. Mater. Chem.* **2003**, *13*, 1023–1029.
27. Frye, C. L.; Vincent, G. A.; Finzel, W. A. Pentacoordinate Silicon Compounds. V. Novel Silatrane Chemistry. *J. Am. Chem. Soc.* **1971**, *93*, 6805–6811.
28. Verkade, J. G. Atranes: New Examples with Unexpected Properties. *Acc. Chem. Res.* **1993**, *26*, 483–489.
29. Cabrera, S.; ElHaskouri, J.; Guillem, C.; Latorre, J.; BeltranPorter, A.; BeltranPorter, D.; Marcos, M. D.; Amoros, P. Generalised Syntheses of Ordered Mesoporous Oxides: The Atrane Route. *Solid State Sci.* **2000**, *2*, 405–420.
30. Zhao, X. S.; Lu, G. Q.; Whittaker, A. K.; Millar, G. J.; Zhu, H. Y. Comprehensive Study of Surface Chemistry of MCM-41 Using ^{29}Si CP/MAS NMR, FTIR, Pyridine-TPD, and TGA. *J. Phys. Chem. B* **1997**, *101*, 6525–6531.
31. Socrates, G. *Infrared and Raman Characteristic Group Frequencies*, 3. ed.; Wiley: New York, 2005.
32. Kang, T.; Park, Y.; Choi, K.; Lee, J. S.; Yi, J. Ordered Mesoporous Silica (SBA-15) Derivatized with Imidazole-Containing Functionalities as a Selective Adsorbent of Precious Metal Ions. *J. Mater. Chem.* **2004**, *14*, 1043–1049.
33. Okabayashi, H.; Izawa, K.; Yamamoto, T.; Masuda, H.; Nishio, E.; O'Connor, C. J. Surface Structure of Silica Gel Reacted with 3-Mercaptopropyltriethoxysilane and 3-Aminopropyltriethoxysilane: Formation of the S-S Bridge Structure and its Characterization by Raman Scattering and Diffuse Reflectance Fourier Transform Spectroscopic Studies. *Colloid Polym. Sci.* **2002**, *280*, 135–145.
34. Thommes, M.; Kohn, R.; Froba, M. Sorption and Pore Condensation Behavior of Nitrogen, Argon, and Krypton in Mesoporous MCM-48 Silica Materials. *J. Phys. Chem. B* **2000**, *104*, 7932–7943.